ARL-TR-9509 ● AUG 2022

DEVCOM ARMY RESEARCH LABORATORY

Investigation of Arbitrary Lagrangian–Eulerian (ALE) Modeling and Alternative Material Formulations of Roma Plastilina Ballistic Clay Using LS-DYNA Numerical Model

by Dmitriy Krayterman

NOTICES

Disclaimers

The findings in this report are not to be construed as an official Department of the Army position unless so designated by other authorized documents.

Citation of manufacturer's or trade names does not constitute an official endorsement or approval of the use thereof.

Destroy this report when it is no longer needed. Do not return it to the originator.

ARL-TR-9509 ● AUG 2022

Investigation of Arbitrary Lagrangian–Eulerian (ALE) Modeling and Alternative Material Formulations of Roma Plastilina Ballistic Clay Using LS-DYNA Numerical Model

Dmitriy Krayterman
DEVCOM Army Research Laboratory

REPORT DOCUMENTATION PAGE

Form Approved
OMB No. 0704-0188

1. REPORT DATE *(DD-MM-YYYY)*	2. REPORT TYPE	3. DATES COVERED (From - To)
August 2022	Technical Report	1 July 2021–1 June 2022

4. TITLE AND SUBTITLE
Investigation of Arbitrary Lagrangian–Eulerian (ALE) Modeling and Alternative Material Formulations of Roma Plastilina Ballistic Clay Using LS-DYNA Numerical Model

5a. CONTRACT NUMBER

5b. GRANT NUMBER

5c. PROGRAM ELEMENT NUMBER

6. AUTHOR(S)
Dmitriy Krayterman

5d. PROJECT NUMBER

5e. TASK NUMBER

5f. WORK UNIT NUMBER

7. PERFORMING ORGANIZATION NAME(S) AND ADDRESS(ES)
DEVCOM Army Research Laboratory
ATTN: FCDD-RLW-TB
Aberdeen Proving Ground, MD 21005-5066

8. PERFORMING ORGANIZATION REPORT NUMBER
ARL-TR-9509

9. SPONSORING/MONITORING AGENCY NAME(S) AND ADDRESS(ES)

10. SPONSOR/MONITOR'S ACRONYM(S)

11. SPONSOR/MONITOR'S REPORT NUMBER(S)

12. DISTRIBUTION/AVAILABILITY STATEMENT
Approved for public release: distribution unlimited.

13. SUPPLEMENTARY NOTES

14. ABSTRACT
A computational study was performed to compare the current finite element analysis model of Roma Plastilina No. 1 clay based on Lagrangian clay element formulation with arbitrary Lagrangian–Eulerian (ALE) element formulation and with alternative ALE material models. The objective of the study was to assess the feasibility of the ALE modeling technique for this application and the accuracy of the various material models combined with the ALE modeling approach.

15. SUBJECT TERMS
clay modeling, clay backing, simulation, finite element analysis, threat intercept, penetrating projectiles, Terminal Effects

16. SECURITY CLASSIFICATION OF:			17. LIMITATION OF ABSTRACT	18. NUMBER OF PAGES	19a. NAME OF RESPONSIBLE PERSON
a. REPORT	b. ABSTRACT	c. THIS PAGE			Dmitriy Krayterman
Unclassified	Unclassified	Unclassified	UU	42	19b. TELEPHONE NUMBER (Include area code) (410) 278-6876

Contents

List of Figures

List of Tables

Acknowledgments

The author would like to thank Dr Timothy Zhang for his contribution to this study.

1. Introduction

To protect the torso from firearm-fired projectiles, Soldiers in a battlefield or law enforcement personnel use body armor. However, even if the penetrating projectile is absorbed, injury can still be sustained due to the deformation of the backface of the body armor. To simulate body armor deformation and the resulting human torso injury, experiments with backing material are conducted. One of the materials that is commonly used as backing material for these experiments is ballistic Roma Plastilina No. 1 clay (RP #1).

Numerical models, or finite element analysis (FEA) models, are developed to better understand the mechanism of the projectile (bullet) penetration of the armor plates as well as the interactions between the internal components of the body armor, backing material, and the penetrating projectile. The results of the models can help improve and optimize the body armor performance as well as to reduce body injuries. The torso injury that occurs as a result of deformation of the body armor due to bullet penetration is also known as behind-armor blunt trauma.

The US Army Combat Capabilities Development Command Army Research Laboratory conducted extensive research on experimental characterization and numerical simulations of ballistic RP #1 clay. The initial experimental material characterization and corresponding numerical modeling work of RP #1, including the details on experimental equipment and setup, results, numerical model development, and simulation results are summarized in Zhang et al.[1]

The numerical model of RP #1 developed by Zhang et al.[1] for the initial RP1 material characterization program was also used in another experimental and modeling study of RP #1 conducted by DEVCOM Army Research Laboratory. This time the study was conducted to evaluate novel material fabrication techniques as well as to study the effects of variation in material and the changes to target geometry on depth of penetration (DOP) and resulting crater formation. The approach and results of this study are published in Graham and Zhang.[2]

This study compares the original numerical model developed by Zhang et al.[1] with models developed using arbitrary Lagrangian–Eulerian (ALE) method to simulate RP #1.

2. Study Objective and the ALE Method Description

2.1 Objective

The objective of this investigation is to

- develop the ALE mesh of the ballistic clay RP #1,
- set up a model using ALE mesh similar to the Lagrangian model of ballistic clay RP #1 developed and validated by Zhang et al.[1] (baseline model),
- select LS-Dyna ALE material models best suited for penetration simulation, and
- conduct ALE simulations and select the most accurate, or the most similar to the baseline, ALE material model in the following model response parameters:
    - projectile DOP
    - time to maximum DOP.

2.2 ALE Method

The simulation of the complex physical processes and interactions such as explosion, fragment formation, or structural penetrations may utilize several different computation methods and element formulations. For high-energy dynamic events, one of the methods commonly used is the fluid-structure interaction (FSI) method. In this method, the parts of the model called "domains" that undergo very severe and fast shape deformations are modeled as "fluid," while other regions that undergo moderate deformation are modeled as "structure." The "fluid" domain is represented in LS-DYNA and other FEA solvers with Eulerian element formulation in which the mesh is fixed, material flows through the mesh as it deforms, and each fixed element contains one or more materials.

The "structure" domain is represented with Lagrangian element formulation in which mesh follows the deformation of the part, each element contains one material, elements and nodes move and deform. The ALE method that combines both Lagrangian and Eulerian element formulations and allows Eulerian elements to move in space is used by the LS-DYNA solver, as well as other advanced FEA solvers to simulate complex FSI events (Fig. 1).

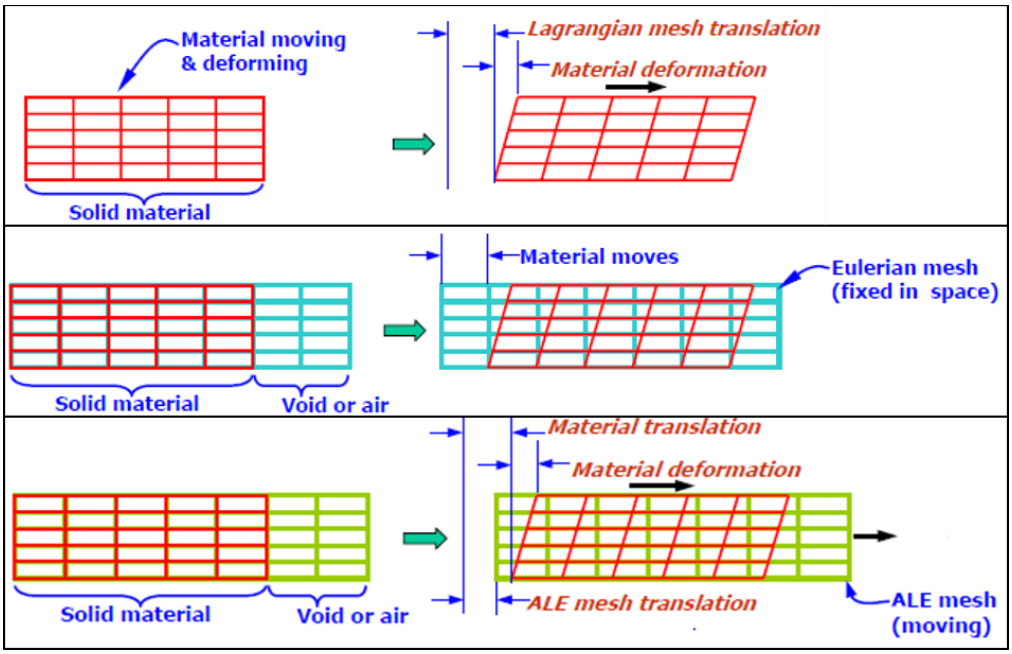

Fig. 1 (Top) Lagrangian, (center) Eulerian, and (bottom) ALE material FEA modeling methods

The clay would be modeled as fluid—the original mesh is fixed and represents the initial volumes of the clay material. This material (clay) is free to move and deform within the fluid (ALE) domain that consists of clay mesh and another Eulerian component-material "air" that is added to allow clay deformation outside of the initial volume. Thus, each Eulerian cell contains a mixture of two materials: clay and air. To simulate material failure, the Lagrangian formulation elements are eroded (deleted) according to material model erosion parameters, and the ALE (Eulerian) formulation elements are replaced with void as they reach specified failure parameters—usually the state of the stress or pressure of the element. So, for the ALE domain the dummy part with *MAT_VACUUM is defined to allow for the void insertion. For this study the material model parameters and properties for the ALE clay were borrowed from publications publicly available on Internet resources and properly mentioned and cited. The model system units for mass, length, time, and temperature are kilogram, centimeter, microsecond, and kelvin (kg, cm, μs, and K), respectively. The detailed ALE model setup and material models and parameters used for each model are described in the corresponding following sections of this report.

3. Baseline Model with Lagrangian Clay

3.1 Model Setup and Material Properties, and Contacts

The original LS-DYNA finite element model developed by Zhang et al.[1] is used as a baseline model for this study. The model simulates a hemispherical-nosed projectile, consisting of hemispherical head (hemi head) and the rod, impacting the clay block. As an approximation, the quarter symmetry was used with appropriate symmetry plane constraints to minimize compute time. Since the clay block rested on a metal frame during the test, the normal displacement on one side of the block was fully constrained to represent the frame. All components were meshed with hexahedral elements; LS-DYNA element formulation 1 (constant stress solid element) was used for all element section properties. The projectile was assigned the impact (initial) velocity of 30.9 m/s (Fig. 2).

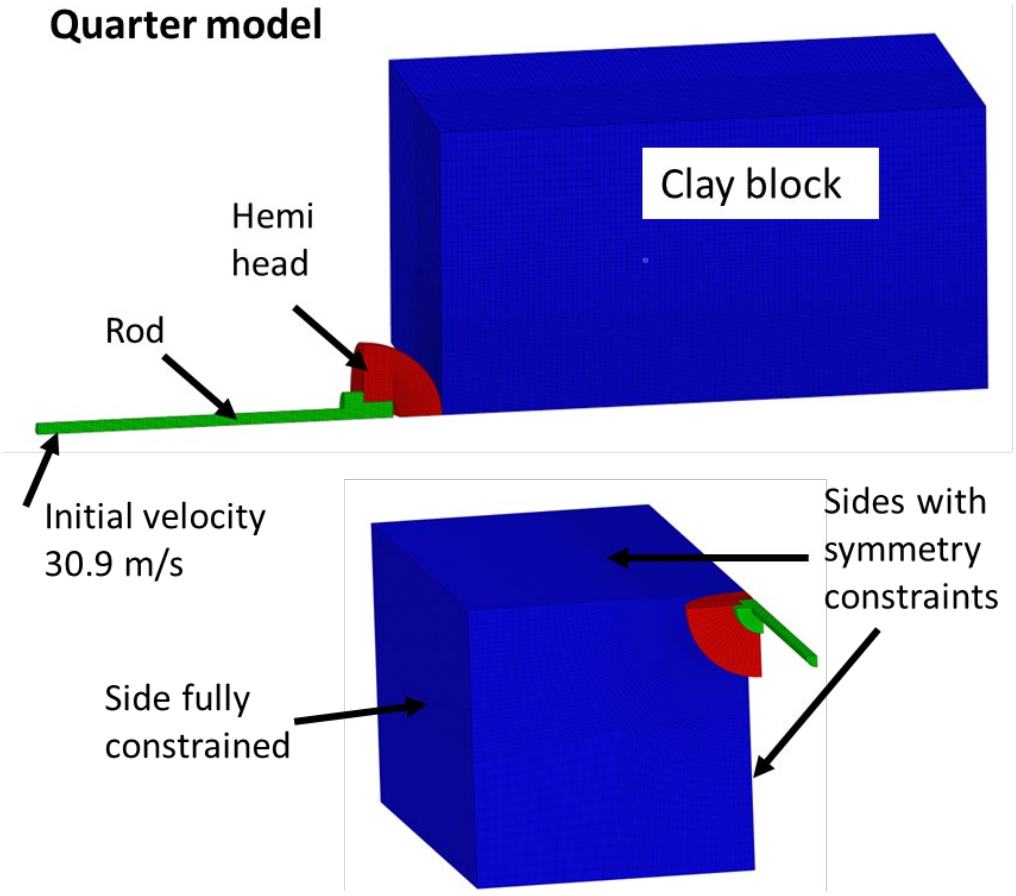

Fig. 2 Baseline finite element model

The material properties for the parts are summarized in Table 1. All material or other (element, section, contact, etc.) parameters specified in tables or LS-DYNA cards in this report are described and explained in the LS-DYNA User Manual.[3]

Table 1 Baseline model LS-DYNA material parameters[3]

Component	Clay block (Lagrangian)							
Material	RP#1							
LS-DYNA Material Card	*MAT_PLASTICITY_COMPRESSION_TENSION (MAT_124)							
LS-DYNA Material Card Parameters	RHO	E	PR	C	P	FAIL	TDEL	
	1342	1.00E+06	0.49				2	
	LCIDC	LCIDT	LCSRC	LCSRT	SRFLAG	LCFAIL	EC	RPCT
	4*	5**	3***	3***	0	0	2.00E+06	1.0
	PC	PT	PCUTC	PCUTT	PCUTF			
	3.00E+02	3.00E+02	1000000	-1.50E+04	0.0			
Component	Hemi head							
Material	Nylon 101							
LS-DYNA Material Card	*MAT_ELASTIC (MAT_1)							
LS-DYNA Material Card Parameters	RHO	E	PR					
	1203.43	2.93E+09	0.39					
Component	Rod							
Material	Delrin							
LS-DYNA Material Card	*MAT_ELASTIC (MAT_1)							
LS-DYNA Material Card Parameters	RHO	E	PR					
	1486	2.41E+09	0.35					

* Load curve ID (LCID) 4 - effective stress vs. effective plastic strain in compression.
** Load curve ID 5 - effective stress vs. effective plastic strain in tension.
*** Load curve ID 3 - load curve ID defining strain-rate scaling factor on yield stress vs. strain rate in compression (LCSRC) or tension (LCSRT).

The material model selected for the clay (RP #1) material requires experimentally developed material characterization curves for stress versus strain in tension, in compression, and for the strain-rate effects if those are present.

Curves for effective stress versus effective plastic strain in compression (curve ID 4) and tension (curve ID 5) are defined in LS-DYNA input with following *DEFINE_CURVE cards:

```
*DEFINE_CURVE
$#     LCID      SIDR       SFA       SFO      OFFA      OFFO    DATTYP
         4         0       1.0    1200.0       0.0       0.0         0

$#     LCID      SIDR       SFA       SFO      OFFA      OFFO    DATTYP
         5         0       1.0    1200.0       0.0       0.0         0
```

For both curves the X-axis scale factor (SFA) is 1.0 and the Y-axis scale factor (SFO) is 1200. The curves themselves (Fig. 3) are inputted as X-Y pairs, where the X-axis is effective plastic strain (unitless) and the Y-axis is effective stress in kilopascals (kPa). Since the model is using metric units—meters, kilogram, seconds (MKS), the kilopascals are converted to pascals with applied scale factor of 1000. Additional scale factor of 1.2 is used to account for temperature effects.[1] Thus, the total SFO of 1200 is applied to both curves.

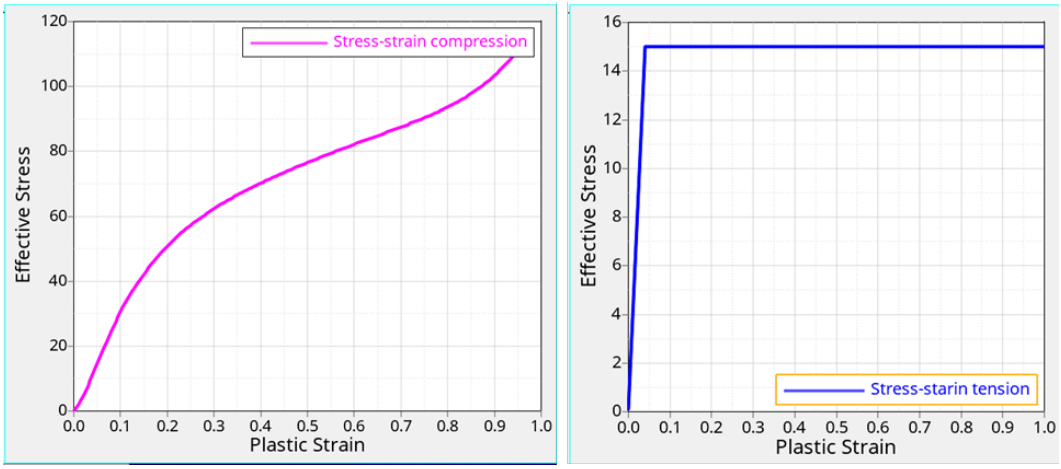

Fig. 3 Clay material effective stress vs. effective plastic strain in compression curve ID 4 (left) and in tension curve ID 5 (right)

The curve for the strain-rate effects, or strain-rate scale factor on yield stress in tension and compression, curve ID 3, is defined with another *DEFINE_CURVE card:

$#	LCID	SIDR	SFA	SFO	OFFA	OFFO	DATTYP
	3	0	1.0	1.0	0.0	0.0	0

The values are inputted as X-Y pairs, where the X-axis is effective strain rate (s^{-1}) and the Y-axis is a strain-rate scale factor on yield stress (unitless) (Fig. 4).

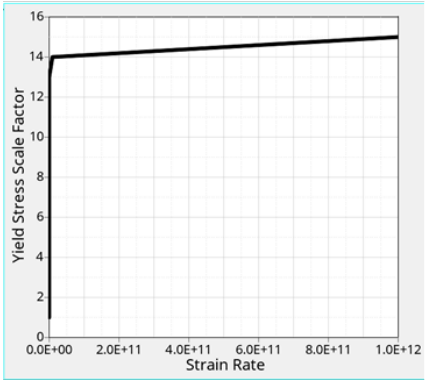

X (strain rate)	Y (scale factor)
0.0	1.0
0.007	1.0
0.07	1.099
0.7	1.255
10	4.00
100	6.00
1000	7.60
1e5	10.20
1e8	13.00
1e10	14.00
1e12	15.00

Fig. 4 Strain-rate scale factor on yield stress (curve ID 3)

The contact between the projectile head and clay that would allow element erosion and friction of 0.19 were assigned using LS-DYNA card *CONTACT_ERODING_SURFACE_TO_SURFACE.

3.2 Baseline Model Simulation Results

The baseline model simulation results are shown at 0 s (initial position), 2 ms, 5 ms (maximum displacement), and 15 ms (end of the simulation) (Fig. 5).

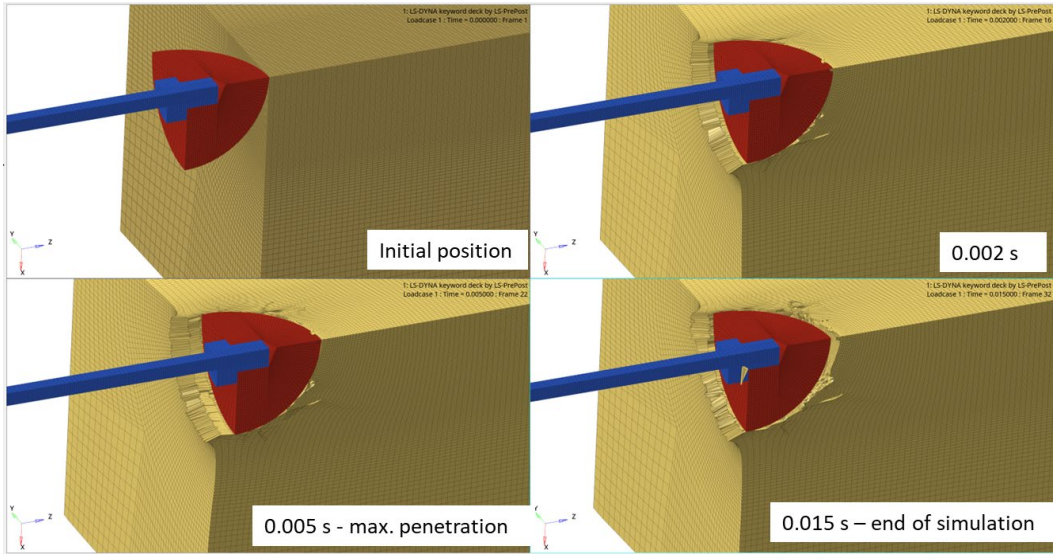

Fig. 5 Baseline model simulation results

The projectile penetration (hemisphere head tip displacement) into the clay block versus time is plotted on Fig. 6. The maximum displacement (penetration) of 51 mm is observed at approximately 5 ms.

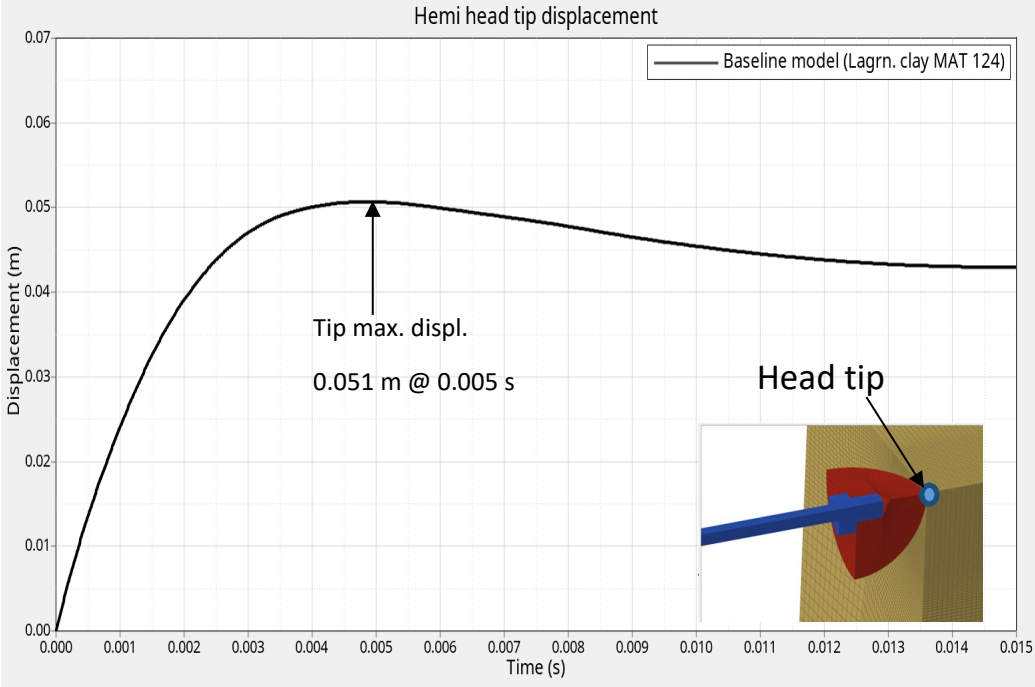

Fig. 6 Projectile head penetration into the clay vs. time

4. "ALE Equivalent" Model

4.1 ALE Equivalent Model Setup

To compare the ALE clay model directly to the baseline Lagrangian clay model, the clay component was remeshed according to the LS-DYNA guidance for meshing ALE parts. The ALE mesh should be made of hexahedral elements with a shape as close to a perfect cube as possible at the regions where high material deformation is expected. The size of ALE elements should be similar to the size of Lagrangian elements with which the contact is expected—in this case, the head of the projectile. Therefore, the mesh of the clay was modified accordingly: near the contact with the projectile head the mesh size was similar to that of the head and away from the contact the mesh size increased (Fig. 7).

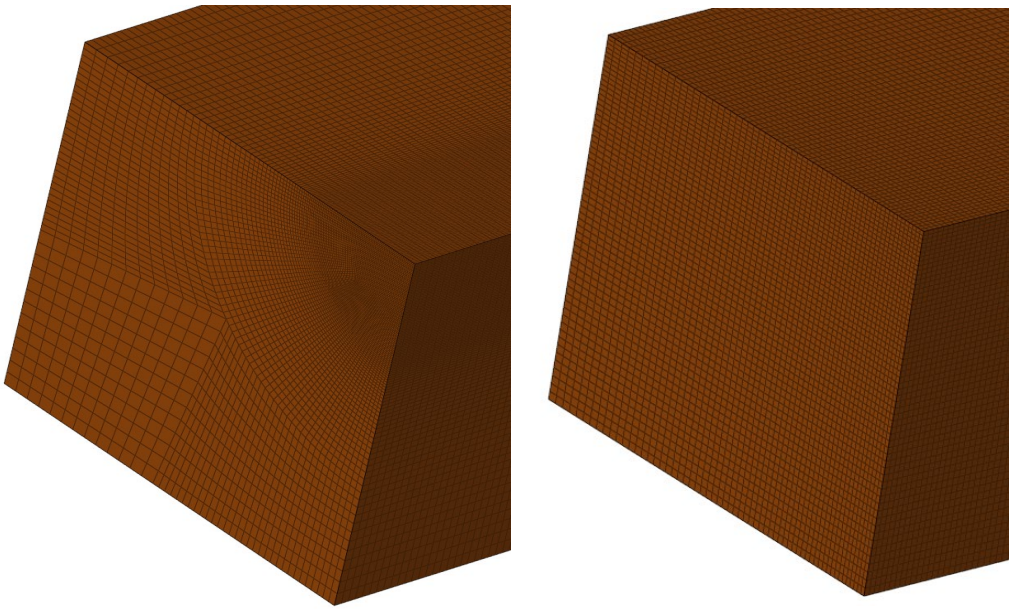

Fig. 7 Original Lagrangian (left) vs. ALE clay block mesh (right)

Also, the mesh for the air component was added to allow clay material to deform/flow into the outside of the initial box shape. The number of elements and nodes (mesh statistics) for the ALE equivalent model as well as for the baseline model is summarized in Table 2.

Table 2 Model mesh statistics summary

Model	Baseline (Lagrangian)	ALE Equivalent		Both (Common Components)		Baseline (Lagrangian) Total	ALE Equivalent Total
Component	Clay	Clay	Air	Hemi head	Rod		
Nodes	592668	375821	454491	21402	22356	636030	854253
Elements	571800	360000	424000	19152	18493	609445	821645

LS-DYNA element formulation 11 (1 point ALE multimaterial element) was used for all ALE (clay, air) element section properties. The clay ALE component was assigned the same material properties (*MAT_PLASTICITY_COMPRESSION _TENSION or MAT_124) as it used in the baseline model. All other parts' (rod and hemispherical head) mesh, section properties, and material properties were kept the same as in the baseline model. Also, the same initial velocities and constraints used in the original model were carried over to the ALE model (Fig. 8).

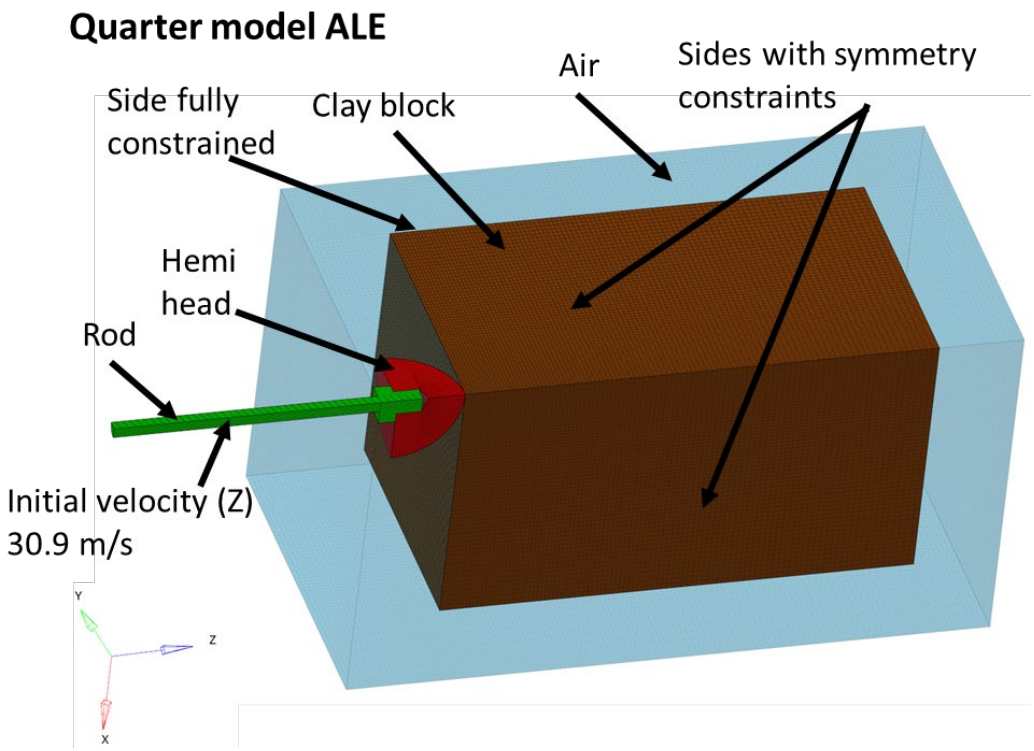

Fig. 8 ALE equivalent finite element model

The material properties for the clay, the hemispherical head, and the rod were carried over from the baseline model (Table 1). The material properties for the newly created components—the air and the vacuum, or void, which are used to replace the failed clay ALE elements as they reach prespecified failure parameters, are summarized in Table 3.

Table 3 ALE equivalent model air and vacuum component LS-DYNA material summary[3,4]

Component	AIR (ALE)							
Material	AIR							
LS-DYNA Material Card	*MAT_NULL							
LS-DYNA Material Card Parameters	RO	PC	Mu					
	1.18	0.00	1.84E-05					
Equasion of State (EOS)	*EOS_LINEAR_POLYNOMIAL							
Equasion of State (EOS) parameters	C0	C1	C2	C3	C4	C5	C6	
	0	0	0	0	0.4	0.4	0	
	E0	V0						
	0	0						
Component	VACUUM (dummy part for void)							
Material	VACUUM							
LS-DYNA Material Card	*MAT_VACUUM							
LS-DYNA Material Card Parameters	RO							
	1.00E-09							

To define the coupling between the Lagrangian (structure) and the ALE (fluid) components, LS-DYNA employs the FSI algorithm. The FSI is a penalty-based algorithm that tracks the relative displacement between fluid and structure, computes penetrations and resulting coupling forces, and then applies computed forces to the interacting nodes. The FSI is controlled by the *CONSTRAINED_LAGRANGE_IN_SOLID card with parameters that allow coupling and interaction between the fluid (clay, air) and the structure (projectile). The baseline model used 0.19 for static and dynamic friction coefficients between the projectile and clay; the same coefficient is used for FSI coupling here. The LS-DYNA card FSI values used in the ALE equivalent model are summarized in Table 4.

Table 4 Clay-projectile coupling parameters summary

LS-DYNA Contact Card	*CONSTRAINED_LAGRANGE_IN_SOLID							
LS-DYNA Contact Card Parameters	slave*	master*	sstyp	mstyp	nquad	ctype	direc	mcoup**
	2	1	0	0	2	4	2	-44
	start	end	pfac	fric	frcmin	norm	normtyp	damp
	0.0	0.0	0.1	0.19	0.0	0	0	0.0
	cq	hmin	hmax	ileak	pleak	lcidpor	nvent	blockage
	0.0	0.0	0.0	0	0.1	0	0	0
	iboxid	ipenchk	intforc	ialesof	lagmul	pfacmm	thkf	
	0	0	1	0	0.0	0	0.0	

* Slave (structure) and master (fluid) part IDs.

** Set ID of the coupled multimaterial group. For this model it includes clay part only.

To summarize, the ALE equivalent model: only clay mesh, clay element type and formulation, and contact definition with the projectile were changed from the original Lagrangian baseline model. All these changes, in addition to adding air and void parts, are essential to convert the clay part to ALE formulation. Thus, the ALE equivalent model is set up to be as close as possible to the original Lagrangian model.

4.2 ALE Equivalent Model Simulation Results

The ALE equivalent model simulation results are shown at 0 s (initial position), 5 ms (maximum penetration), 12 ms (maximum rebound), and 15 ms (end of the simulation) (Fig. 9).

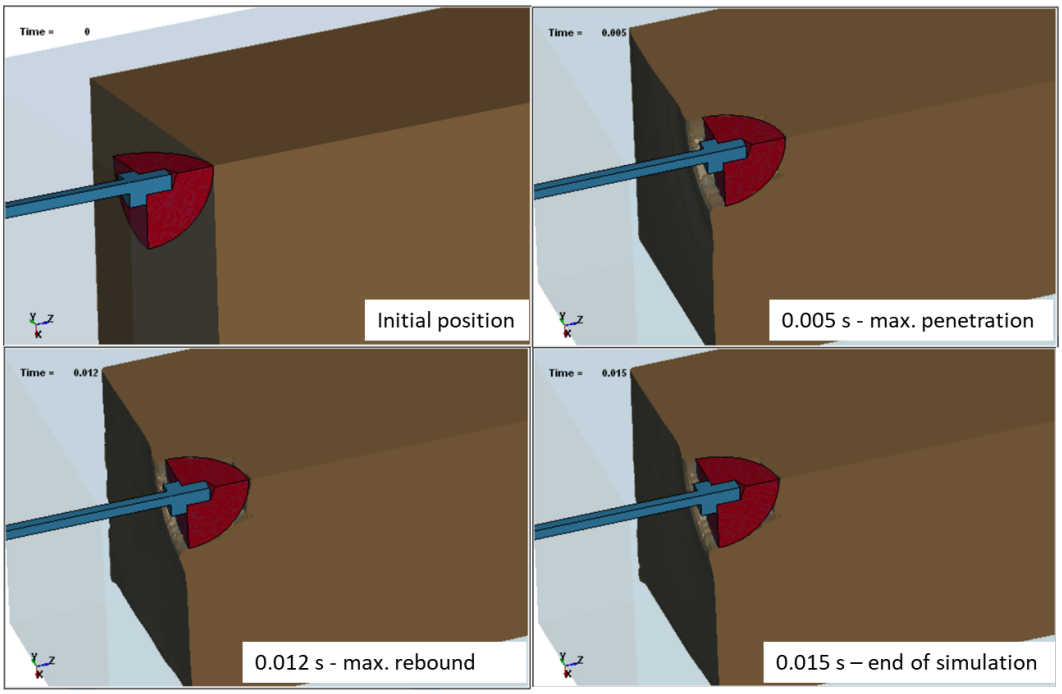

Fig. 9 ALE equivalent model simulation results

After maximum rebound the projectile is pushed slightly forward because it is being pushed back by clay material from behind the head (Fig. 10).

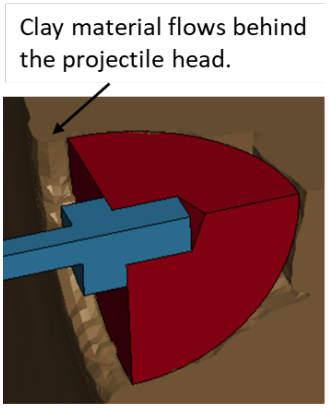

Fig. 10 Clay material behind the projectile head at maximum rebound

The projectile penetration into the clay block for the ALE equivalent model and the baseline model versus time are plotted on Fig. 11. The maximum penetration of 50 mm is observed at approximately 5 ms for the ALE equivalent model compared to 51 mm for the baseline model.

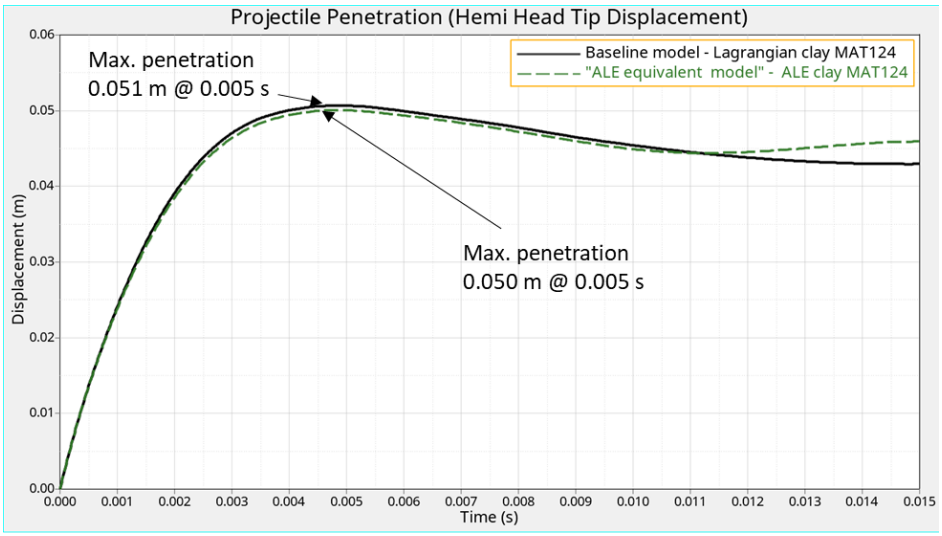

Fig. 11 ALE equivalent model vs. baseline model projectile penetration into the clay

4.3 Observations and Discussion

The ALE equivalent model is almost identical to the baseline model in terms of the projectile's maximum penetration distance and timing. The slight recovery (~3 mm) from the maximum rebound that happens after 11 ms is due to the elastic material flowing behind the head and pushing forward.

5. Alternative Clay Material Models

The objective of this study, as stated previously, is to investigate the alternative ALE material models for clay available in LS-DYNA and compare alternative material simulation results with the baseline simulation results. Many ALE material models are implemented in LS-DYNA; however, according to the LS-DYNA user manual,[3] only 10 are validated. The validated materials model for ALE simulations are marked "8A" in the LS-DYNA user manual[3] and they are as follows:

*MAT_001: *MAT_ELASTIC [0,1H,1B,1I,1T,2,3a,3c,5,8A]

*MAT_003: *MAT_PLASTIC_KINEMATIC [0,1H,1I,1T,2,3a,3c,5,8A]

*MAT_005: *MAT_SOIL_AND_FOAM [0,5,3c,8A]

*MAT_008: *MAT_HIGH_EXPLOSIVE_BURN [0,5,3c,8A]

*MAT_009: *MAT_NULL [0,1,2,3c,5,8A]

*MAT_015: *MAT_JOHNSON_COOK [0,2,3a,3c,5,8A]

*MAT_024: *MAT_PIECEWISE_LINEAR_PLASTICITY [0,1H,2,3a,3c,5,8A]

*MAT_140: *MAT_VACUUM [0,8A]

*MAT_148: *MAT_GAS_MIXTURE [0,8A]

*MAT_238: *MAT_PERT_PIECEWISE_LINEAR_PLASTICITY [0,1H,2,3,5,8A]

Some of the validated materials are developed to simulate explosive materials and/or fluid materials (such as air, vacuum, water, etc.) and are not appropriate to simulate clay with. Several material models that are appropriate to be used for clay are selected as alternatives for this study:

*MAT_003: *MAT_PLASTIC_KINEMATIC

*MAT_005: *MAT_SOIL_AND_FOAM

*MAT_015: *MAT_JOHNSON_COOK

*MAT_024: *MAT_PIECEWISE_LINEAR_PLASTICITY

The previous material models were investigated as alternatives to that of the baseline (*MAT_124: *MAT_PLASTICITY_COMPRESSION_TENSION), which is not in the list of LS-DYNA validated ALE material models. Only clay ALE material models were modified in the alternative material model study. All other model parameters (such as mesh, constraints, initial velocity, projectile material, etc.) were kept the same as in the ALE equivalent model.

5.1 Alternative Clay Material Model 1: *MAT_PLASTIC_KINEMATIC (MAT03)

5.1.1 Material Model Description

This material model is suited to model isotropic and kinematic hardening plasticity with the optional rate effects. The strain-rate effects are accounted for by using the Cowper–Symonds model that scales the yield stress with the factor

$$1 + (\dot{\varepsilon}/C)^{1/p}$$

where $\dot{\varepsilon}$ is the strain rate, and C and p are strain-rate parameters for the Cowper–Symonds strain-rate model.[3]

The material parameters were obtained from Buchely et al.,[5] in which the authors developed the Cowper–Symonds model parameters from static and dynamic tests

of RP #1. For the dynamic test, the range of initial velocities was between 20 and 43 m/s.[5]

The quasi-static and dynamic test material model parameters are summarized in Tables 5 and 6, respectively.

Table 5 Cowper–Symonds materials parameters of RP clay from quasi-static tests[5]

Elastic modulus	Cowper–Symonds parameters		
(E)	(Y_0)	(D)	(q)
1.73 MPa	0.08 MPa	0.9192s^{-1}	9.034

Table 6 Dynamical parameters (D.P.) of RP #1 determined with DI test and inverse method[5]

Run	E (MPa)	Y_0 (MPa)	D (s^{-1})	q (–)
1	11.83	0.153	0.172	6.99
2	11.89	0.153	0.197	7.00
3	11.32	0.153	0.180	7.00
4	11.42	0.153	0.184	6.99
5	11.88	0.153	0.197	6.99
6	11.47	0.153	0.174	7.00
7	11.95	0.153	0.163	6.99
8	10.93	0.152	0.181	6.97
9	11.98	0.153	0.168	7.00
10	11.70	0.153	0.199	7.00
Mean	***11.64***	***0.153***	***0.181***	***6.99***
St. Dev.	*0.34*	*<0.001*	*0.013*	*<0.01*
Upper 95% C.I.	*11.882*	*0.1531*	*0.1904*	*6.998*
Lower 95% C.I.	*11.392*	*0.1527*	*0.1714*	*6.985*

The D and q parameters from Tables 5 and 6 correspond to C and p parameters for the LS-DYNA material model, respectively. For the dynamic material model, the mean row material values were used in the simulation. The LS-DYNA material card values, converted into appropriate unit system (MKS) for quasi–static and dynamic material models, are summarized in Table 7.

Table 7 Alternative material model 1 (Mat 03) LS-DYNA material parameters

Component	Clay block (ALE)							
Material	RP#1							
LS-DYNA Material Card	MAT_PLASTIC_KINEMATIC (MAT03)							
LS-DYNA Material Card Quasi - Static Parameters	RHO	E	PR	SIGY	ETAN	BETA		
	1529	1.73E+06	0.43	80000.0		0.0		
	SRC	RP	FS	VP				
	0.9192	9.034	2.0	1.0				
LS-DYNA Material Card Dynamic Parameters	RHO	E	PR	SIGY	ETAN	BETA		
	1529	1.16E+07	0.43	153000.0		0.0		
	SRC	RP	FS	VP				
	0.181	6.99	2.0	1.0				

5.1.2 Simulation Results

The ALE alternative model 1 visual simulation results for quasi-static and dynamic material model simulations are shown in Fig. 12.

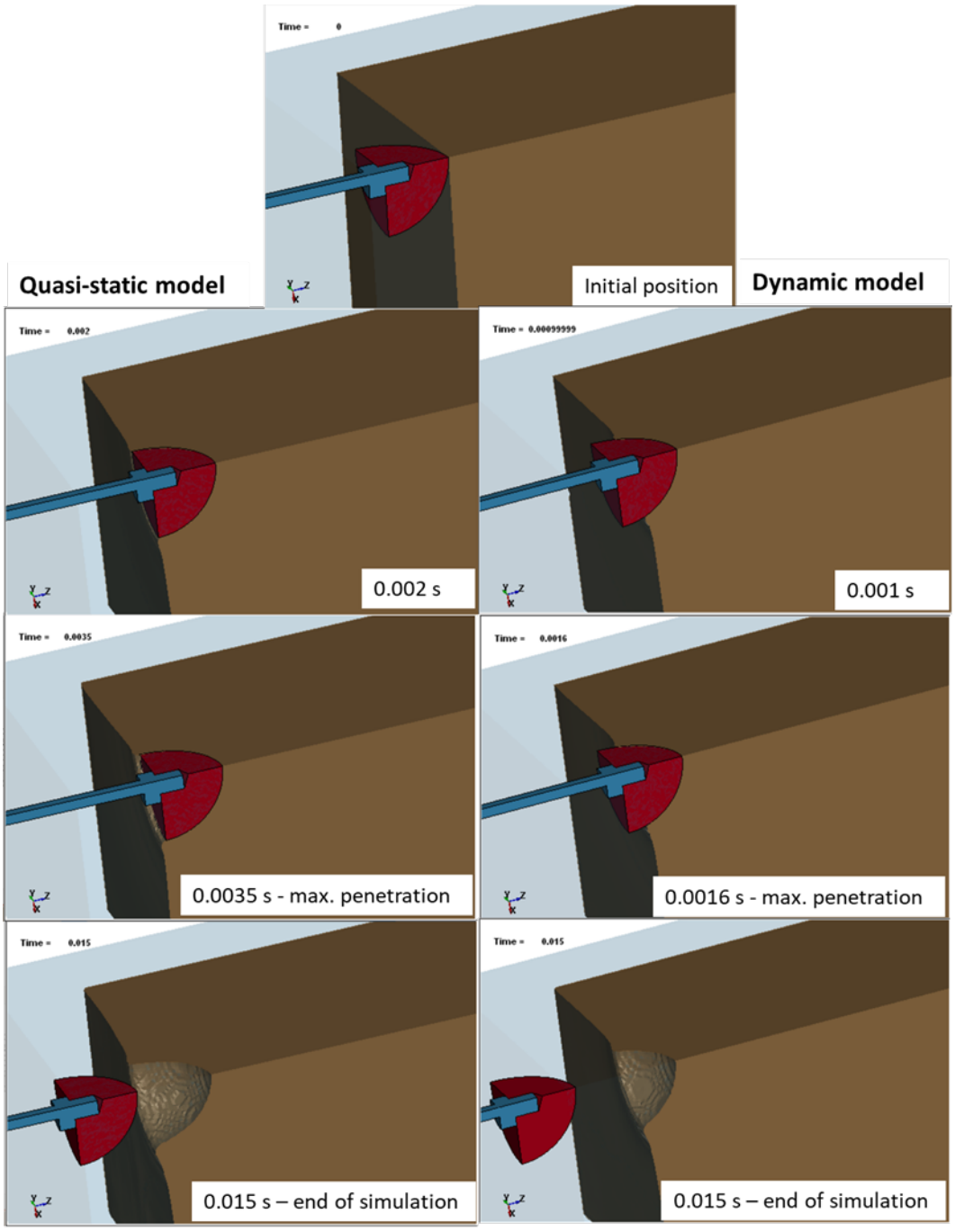

Fig. 12 ALE alternative model 1 quasi-static (left) and dynamic (right) material model simulation results

The plots of projectile penetration into the clay block for alternative material model 1 quasi-static and dynamic models versus the baseline (Lagrangian) model are shown in Fig. 13.

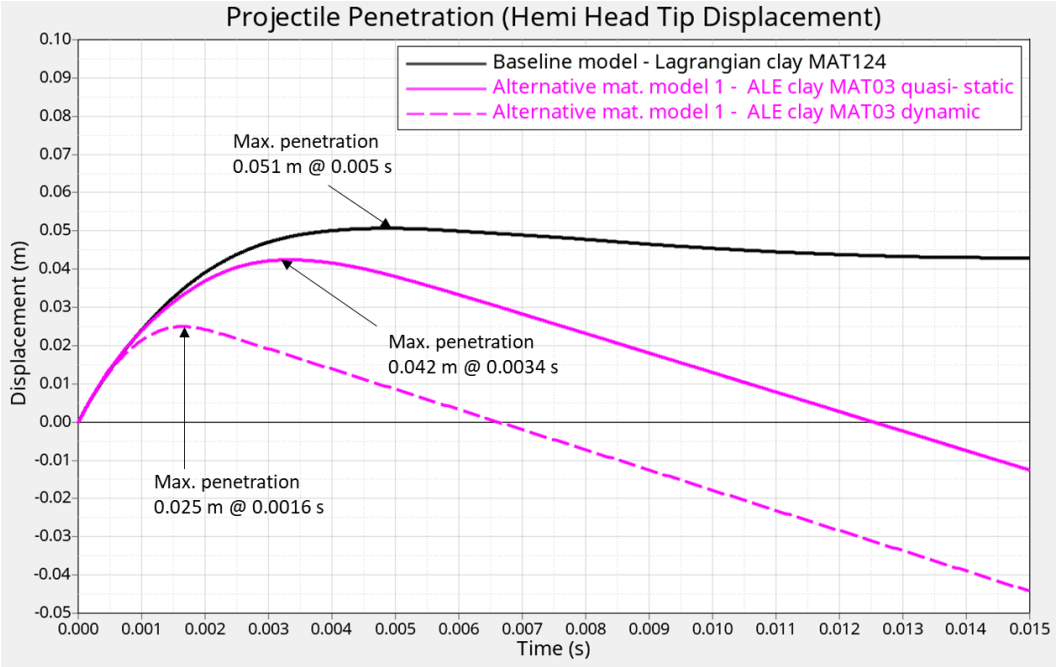

Fig. 13 ALE alternative model 1 (quasi-static and dynamic) vs. baseline model projectile penetration into the clay

5.1.3 Observations and Discussion

The quasi-static material model penetration response is much closer in DOP (42 mm quasi-static vs. 51 mm baseline) and timing to maximum penetration (3.4 ms vs. 5 ms) to the baseline than that of a dynamic model. Obviously, the impact velocity (30.9 m/s) of the penetrator in this case and resulting loading of the clay block is better modeled with quasi-static material model assumptions than dynamic model assumptions. The rebound for both models, quasi-static and dynamic, is significantly larger than what was observed in the baseline model, which signifies more incompressibility of the material model.

Overall, since the main modeling objective is matching the experimental depth and timing of penetration while the rebound response is not so important, the quasi-static material model could be an acceptable alternative material model for the impact velocities around 30 m/s. Additional study may need to be conducted to verify how high the impact velocity could be for the quasi-static model to be within reasonable correlation to the baseline model response.

5.2 Alternative Clay Material Model 2: *MAT_SOIL_AND_FOAM (MAT05)

5.2.1 Material Model Description

This material model is commonly used to represent soil, concrete, or crushable foam. The model uses pressure as a function of volumetric strain to simulate deformation of soil material. The pure RP #1 clay may not contain other soil components such as sand and minerals and may not accurately represent the moisture content of a soil. However, as a first approximation, the accuracy of the model may be sufficient to provide a feasible alternative material model for RP #1.

The material parameters for clay soil were obtained Busch and Tarefder.[6] The material model was used for finite element simulations of an explosive air blast on clay soil in LS-DYNA using ALE methodology. The clay material input parameters for LS-DYNA MAT05 formulation, including the pressure as function of volumetric strain, are listed in Tables 8 and 9.

Table 8 Strength and stiffness properties of clayey soils used in experiment[6]

Parameter	Result
Cohesion, c	0.021 MPa
Friction angle, φ	4.0°
Elastic modulus, E	7.57 MPa
Poisson's ratio, v	0.49973
Shear modulus, G	2.524 MPa
Saturated bulk modulus, K	4673 MPa
Soil skeleton bulk modulus, K_s	355 MPa
Mineral grain bulk modulus (Kaolinite), K_g	49,000 MPa

Table 9 Input parameters for soil and foam material model (LS-DYNA Model 5)[6]

Parameter	Input
Yield function constant, a_0	0.001 MPa^2
Yield function constant, a_1	0.0049 MPa
Yield function constant, a_2	0.0079
Tensile pressure cutoff, P_c	–0.05 MPa
Compressibility curve inputs	
Pressure, P (MPa)	Volume strain, ε_{log}
0.0	0.0000
100.0	–0.0216
200.0	–0.0437
400.0	–0.0895
600.0	–0.1374
800.0	–0.1878
1000.0	–0.2408
2000.0	–0.5586
3000.0	–1.0272
4000.0	–1.9380

The corresponding LS-DYNA material card values, converted into appropriate unit system (MKS), are summarized in Table 10.

Table 10 Alternative material model 2 (Mat 05) LS-DYNA material parameters

Component	Clay (ALE)							
Material	RP#1							
LS-DYNA Material Card	*MAT_SOIL_AND_FOAM (MAT_05)							
LS-DYNA Material Card Parameters	RHO	G	BULK	A0	A1	A2	PC	
	1570	2.52E+06	4.67E+09	1.00E+09	4900	0.0079	-50000.0	
	VCR	REF	LCID					
	0							
	EPS1	EPS2*	EPS3	EPS4	EPS5	EPS6	EPS7	EPS8
	0	0.0216	0.0437	0.0895	0.1374	0.1878	0.2408	0.5586
	EPS9	EPS10						
	1.0272	1.938						
	P1	P2	P3	P4	P5	P6	P7	P8
	0	1.00E+08	2.00E+08	4.00E+08	6.00E+08	8.00E+08	1.00E+09	2.00E+09
	P9	P10						
	3.00E+09	4.00E+09						

* A negative sign is applied internally to the absolute value of each entry of volumetric strain.

5.2.2 Simulation Results

The ALE alternative model 2 – clay material model soil and foam (MAT05) visual simulation results for are shown in Fig. 14.

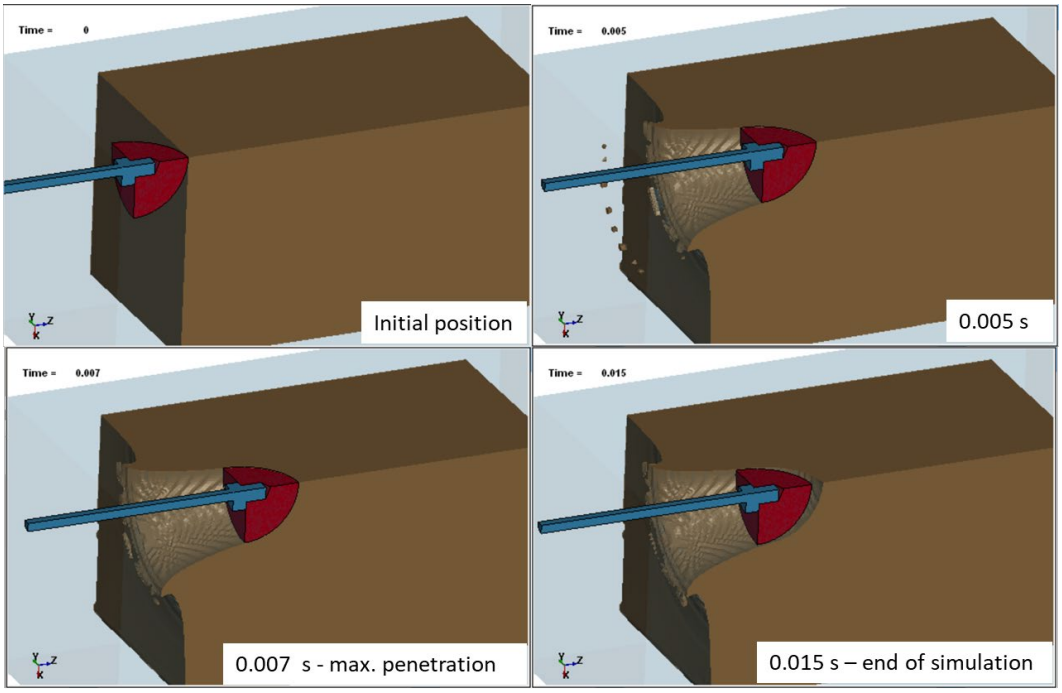

Fig. 14 ALE alternative model 2 – soil and foam clay material model simulation results

The projectile penetration into the clay block for alternative material model 2 versus the baseline (Lagrangian) model plots are shown in Fig. 15.

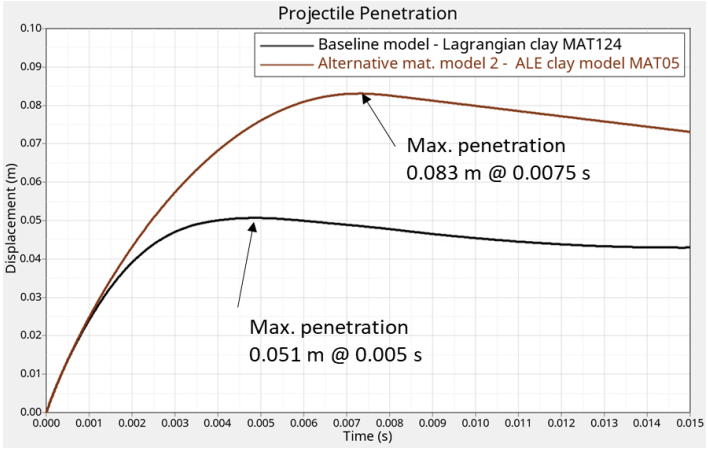

Fig. 15 ALE alternative model 2 vs. baseline model projectile penetration into the clay

5.2.3 Observations and Discussion

The alternative material model 2 indicates significantly higher maximum penetration and timing to maximum than that of the baseline, indicating softer material. Since material properties used for the simulation are based on actual soil material characterization, they (material properties) may not accurately represent the pure RP #1. This may be corrected by assigning a scale factor to the stress–strain curve that will effectively strengthen the material to match the baseline model response. The value of the scale factor could be derived from the optimization analysis that uses the baseline model response as an objective function and a scale factor as a variable.

5.3 Alternative Clay Material Model 3: *MAT_JOHNSON_COOK (MAT15)

The Johnson–Cook (JC) material model is implemented by LS-DYNA to model materials with strain- and temperature-sensitive elasto-plasticity or visco-plasticity where the strain rates vary over a large range and temperature increases due to plastic heating may cause material softening. This material model could be used to simulate ballistic penetrations and resultant deformations claylike materials under different impact conditions with strain-hardening, strain-rate, and thermal effects.

5.3.1 Material Model Description

The JC material model expresses the flow stress (σ_f) as function of the equivalent plastic strain ε_p, equivalent plastic strain rate $\dot{\varepsilon}_p$, and temperature T:

$$\sigma_f = (A + B\varepsilon_p^n)\left(1 + C\ln\frac{\dot{\varepsilon}_p}{\dot{\varepsilon}_p^o}\right)\left[1 - \left(\frac{T - T_o}{T_m - T_o}\right)^m\right]$$

where

A, B, C, n, and m are material input constants.

$\dot{\varepsilon}_p^0$ is the quasi-static strain, and T_0 and T_m are the reference (room) and melting temperatures, respectively.

The material parameters for this model were obtained from Gad and Gao.[7] The publication provides the sources or methods of derivation of material model values that seemed to be sound and applicable for this study. Some of the constants were determined based on the DEVCOM ARL clay characterization experiments,[1] and others were taken from Mates et al.,[8] which determined the RP #1 material parameters of the JC model for reference strain rate of 0.118 s^{-1} and reference temperature of 23 °C.

Tables 11–13 include material model values extracted from Gad and Gao[7]: the elastic and thermal properties of the RP #1 clay (Table 11), the JC model material constants with corresponding temperatures and strain rates used to develop these constants (Table 12), and the constants for the polynomial equation of state (EOS) (Table 13).

Table 11 Elastic and thermal properties of RP #1 clay[7]

E (MPa)	ν	λ (W × m^{-1} × °C^{-1}	c_p (J × kg^{-1}× °C^{-1})	ρ (kg × m^{-3})
168.0	0.49	0.6	1280	1570

Table 12 Constants in the J-C model for RP #1 clay[7]

A (kPa)	B (kPa)	C	m	N
0.01	238.0	0.25	0.502	0.29

Table 13 Constants in the polynomial EOS for RP #1 clay[7]

c_1 (GPa)	c_2 (GPa)	c_3 (GPa)	c_4	c_5	c_6
2.804	40.7	–36.0	1.7	1.7	0

The LS-DYNA material card parameters, converted into appropriate unit system (MKS) for JC material model, are summarized in Table 14.

Table 14 LS-DYNA material card parameters for JC material model

Component	CLAY (ALE)							
Material	RP #1							
LS-DYNA Material Card	*MAT_JOHNSON_COOK (*MAT_15)							
LS-DYNA Material Card Parameters	RHO	G	E	PR				
	1570.0		1.68E+08	0.49				
	A	B	n	C	m	Tm	Tr	EPS0
	10.0	238000.0	0.29	0.25	0.502	100	23	0.118
	Cp	Pc	Spall	IT	d1	d2	d3	d4
	1.28E+03							
	d5							
Equasion of State (EOS)	*EOS_LINEAR_POLYNOMIAL							
Equasion of State (EOS) parameters	C0	C1	C2	C3	C4	C5	C6	
	0	2.80E+09	4.07E+10	-3.60E+10	1.7	1.7	0	
	E0	V0						

5.3.2 Simulation Results

The ALE alternative model 3 – clay material model JC (MAT15) visual simulation results are shown in Fig. 16.

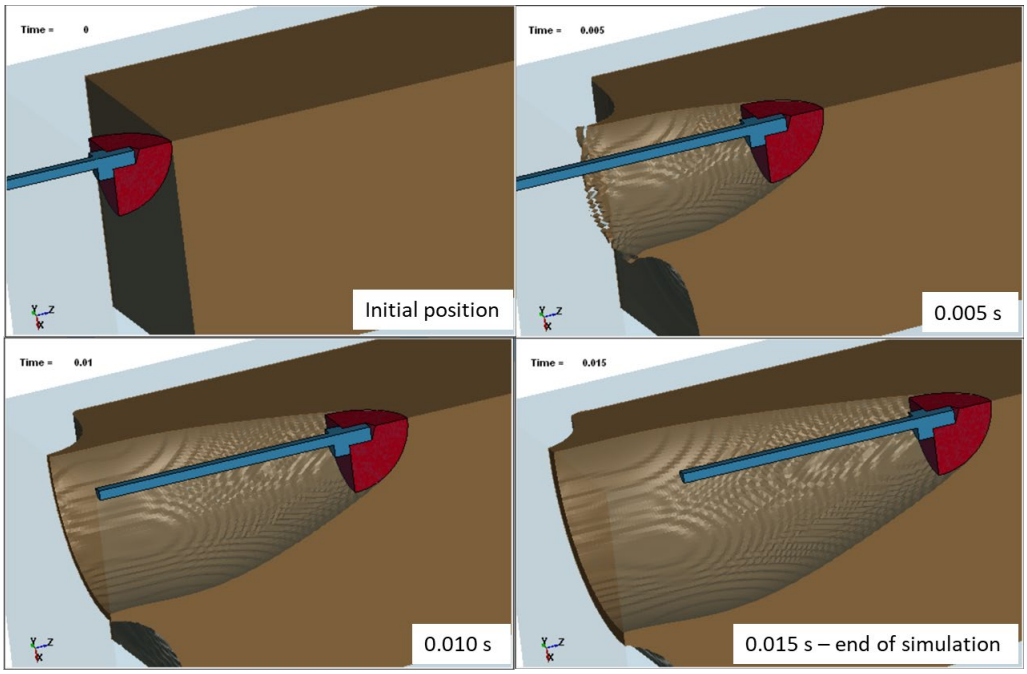

Fig. 16 ALE alternative model 3 – JC clay material model simulation results

The projectile penetration into the clay block for alternative material model 3 versus the baseline (Lagrangian) model results are plotted in Fig. 17.

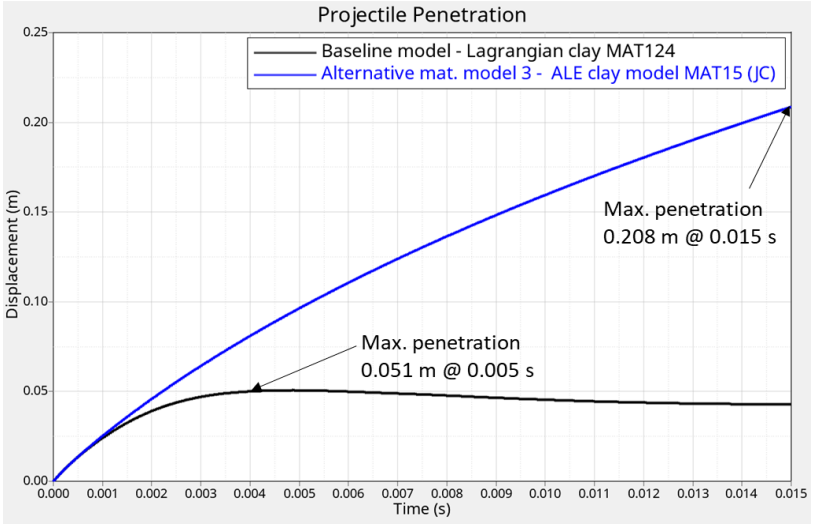

Fig. 17 ALE alternative model 3 vs. baseline model projectile penetration into the clay

5.3.3 Observations and Discussion

The model does seem fit to predict projectile penetration for the simulated conditions. Numerous simulations were completed utilizing various material parameters for this model in an effort to improve model response correlation to the baseline. None of the attempts yielded significant changes in a response curve trend compared to the initial alternative model 3 material parameters. Additional investigation is required to determine the reason why this material model and parameters do not show the trend similar to the one of the baseline model.

5.4 Alternative Clay Material Model 4: *MAT_PIECEWISE_LINEAR_PLASTICITY (MAT24)

5.4.1 Material Model Description

The material type 24 is an elasto-plastic material model that requires a stress–strain curve and allows strain-rate dependency. The strain-rate dependency is accounted for with the load curve defining strain-rate scaling effect on yield stress similar to the MAT124 (baseline) formulation.

Since most of the clay deformation occurs in compression, the compression stress–strain curve (curve ID 4, Fig. 3) from material 124 (baseline) was used to define elasto-plastic behavior. Similarly, the curve ID 3 from material 124 (Fig. 4) was used to define the strain-rate scale factor on yield stress to account for the strain-rate effects. Other material values, such as density, Young's modulus, Poisson's ratio, were borrowed from alternative clay material model 1 (MAT03) parameters.

The LS-DYNA material card parameters for MAT24 material model are summarized in Table 15.

Table 15 LS-DYNA material card parameters for MAT24 material model

Component	Clay (ALE)							
Material	RP#1							
LS-DYNA Material Card	*MAT_PIECEWISE_LINEAR_PLASTICITY (MAT_24)							
LS-DYNA Material Card Parameters	RHO	E	PR	SIGY*	ETAN	FAIL	TDEL	
	1529	1.73E+06	0.43	80000			0.0	
	C	P	LCSRC**	LCSRT**	VP			
	0	0	4	3				

* Value is ignored as material model follows specified material curves.

** Material curves are the same as for material 124 (baseline).

5.4.2 Simulation Results

The ALE alternative model 4 – clay material model MAT_PIECEWISE_LINEAR_PLASTICITY (MAT24) visual simulation results are shown in Fig. 18.

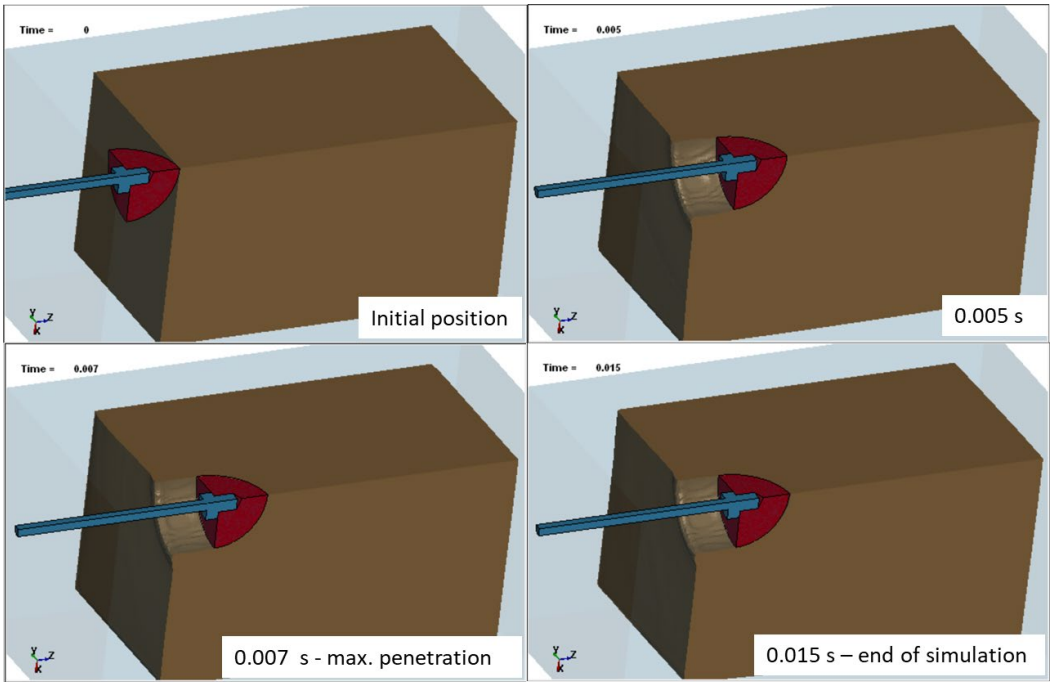

Fig. 18 ALE alternative model 4 – MAT24 clay material model simulation results

The results of the projectile penetration into the clay block for alternative material model 4 versus the baseline (Lagrangian) model are plotted in Fig. 19.

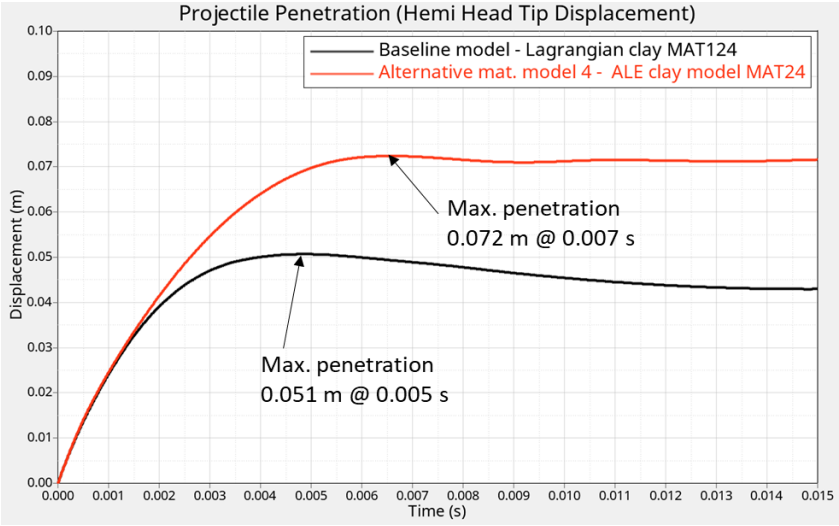

Fig. 19 ALE alternative model 4 vs. baseline model projectile penetration into the clay

5.4.3 Observations and Discussion

The alternative material model 4 indicates higher maximum penetration and timing to maximum than that of the baseline, indicating softer material. The model response is similar to that of the alternative material model 2 (*Mat_Soil_And_Foam). Similar to the alternative material model 2, this correlation could be improved by assigning a scale factor to the stress–strain curve that will match the baseline model response. The value of the scale factor could be obtained from the optimization analysis.

6. Simulation Results Summary

The 15-ms simulations for all models were completed on DOD high-performance computer servers using 48 CPUs, LS-DYNA Release 971, version MPP d R10.1.0.

The projectile penetrations into the clay block for the baseline, ALE equivalent model, and all alternative material models are plotted on Fig. 20.

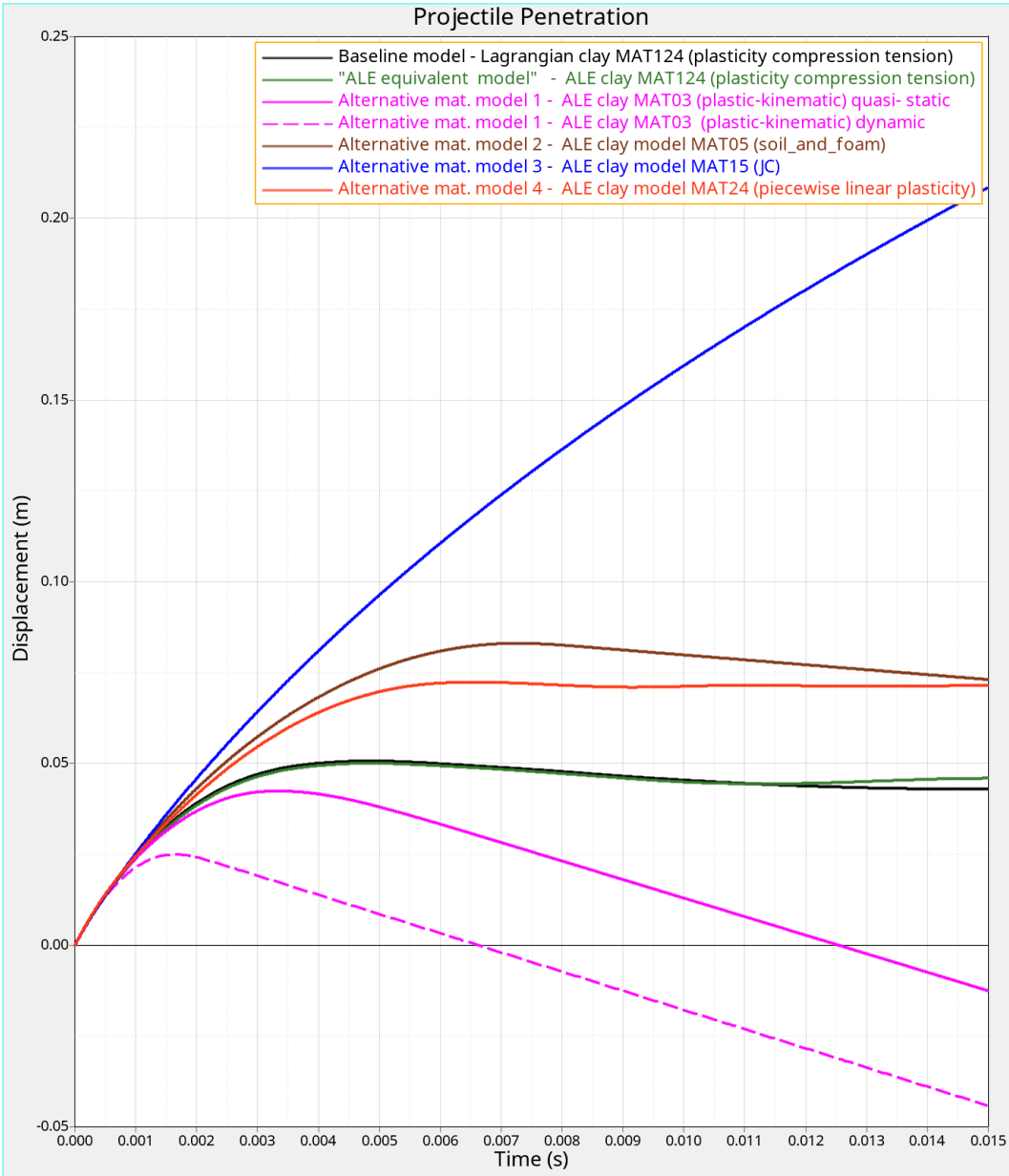

Fig. 20 Projectile penetration into the clay vs. time for all simulations

The comparison between simulated material models summarizing model response parameters such as maximum projectile penetration, time to maximum penetration, as well as percentage difference between the ALE models and the baseline, and computation times for all simulations are summarized in Table 16.

Table 16 Model response summary and compute time for all simulations

Model		Clay element formulation	Clay LS-DYNA material model	Max. Projectile Penetration (mm)	Difference to baseline, %	Time to Max. projectile penetration (ms)	Difference to baseline, %	15 ms simulation time on HPC using 48 cores
Baseline		Lagrang.	MAT124	51	N/A	5.0	N/A	less than 1hr
ALE equivalent		ALE	MAT124	50	-2.0	5.0	0.0	18-20 hrs
Alternative matl 1	quasi-static	ALE	MAT03	42	-17.6	3.4	-32.0	
	dynamic	ALE	MAT03	25	-51.0	1.6	-68.0	
Alternative matl 2		ALE	MAT05	83	62.7	7.5	50.0	
Alternative matl 3		ALE	MAT15	208	307.8	15.0	200.0	
Alternative matl 4		ALE	MAT24	72	41.2	6.5	30.0	

7. Conclusions and Observations

The baseline numerical model was compared to the ALE equivalent numerical model as well as to the alternative ALE material models. The following conclusions and observations could be drawn based on the results of this study:

- All ALE models require significantly more computational resources (up to 20 h of compute time vs. less than 1 h) than the baseline model.
- The ALE equivalent model is almost identical to the baseline model in terms of projectile's maximum penetration distance and timing. It is the best ALE model to be used as the substitute of Lagrangian (baseline) model for the similar range of impact velocities even though the ALE material model (MAT124) is not validated by LS-DYNA.
- Alternative 1 quasi-static material model could also be used in place of the baseline as the DOP and timing to maximum penetration are somewhat similar to the baseline. However, the rebound is significantly larger than that of the baseline model due to higher incompressibility of the material model.
- Alternative material models 2 and 4 both indicate significantly higher maximum penetration and timing to maximum penetration than that of the baseline due to softer material properties. However, the trends of the projectile penetration curves are similar to that of the baseline. In both cases, assigning an appropriate scale factor to the stress–strain curves used for either material model could significantly improve the correlation to the baseline model response. After the scale factor application both models could very well be used in place of the baseline for the similar range of impact velocities.

- Alternative material model 3 does seem useful to predict projectile penetration for the simulated conditions due to the trend of the response curve being completely inconsistent compared to the baseline.

8. Recommendations

Based on the study results the model usage recommendations are as follows:

- Use baseline (Lagrangian) model of RP #1 clay if possible due to relative simplicity to create and incorporate into larger assembly, reduced computational time, smaller model size (number of nodes and elements), and reduced computational time
- Use ALE alternative model if baseline fails due to the high clay element negative volume and/or deformation/distortion because of general deficiencies of the Lagrangian material formulation. While implementation of the material erosion makes the execution failure less likely, especially using the recent execution code versions, it is still possible to encounter such failures during high and fast material distortion events.
- Conduct another computational study to develop scale factors for alternative material models 2 and 4 to match the baseline model response.
- Validate/verify all ALE model predictions against experimental data for the entire applicable impact velocity range and rates of deformation.

9. References

1. Zhang TG, Ivancik J, Mrozek RA, Satapathy SS. Material characterization of ballistic Roma Plastilina No. 1 clay. 30th International Symposium on Ballistics. 2017 Sep 11–15; Long Beach, CA. DOI: 10.12783/ballistics2017/17041.

2. Graham MJ, Zhang TG. Finite element analysis of geometric effects on ballistic clay backing material. CCDC Army Research Laboratory (US); 2019 Sep. Report No.: ARL-TR-8805.

3. [LSTC] Livermore Software Technology Corporation. LS-DYNA keyword user's manual: volumes I–II. LSTC, Inc.; 2018.

4. Tabiei A. EOS tutorial. Unpublished training notes. 2004 May.

5. Buchely MF, Maranon A, Silberschmidt VV. Material model for modeling clay at high strain rates. International Journal of Impact Engineering. 2016;90:1–11. https://doi.org/10.1016/j.ijimpeng.2015.11.005.

6. Busch CL, Tarefder RA. Evaluation of appropriate material models in LS-DYNA for MM-ALE finite element simulations of small-scale explosive airblast tests on clay soils. Indian Geotech J. 2017;47:173–186. https://doi.org/10.1007/s40098-016-0196-4.

7. Gad AI, Gao X-L. Modeling of deformations of Roma Plastilina # 1 clay in column-drop tests by incorporating the coupled strain rate and temperature effects. Mech Adv Mater Struct. 2020;27:13. DOI:10.1080/15376494.2020.1712629.

8. Mates S, Forster A, Riley M, Price K. Mechanical behavior of ballistic clay as a function of temperature, pressure and strain rate. Personal Armour Systems Symposium; 2014 Sep 8–12; Cambridge, United Kingdom. p. 8–12.

List of Symbols, Abbreviations, and Acronyms

ALE	arbitrary Lagrangian-Eulerian
ARL	Army Research Laboratory
CPU	central processing unit
DEVCOM	US Army Combat Capabilities Development Command
DOD	Department of Defense
DOP	depth of penetration
EOS	equation of state
FEA	finite element analysis
FSI	fluid-structure interaction
JC	Johnson-Cook
LSTC	Livermore Software Technology Corporation
MKS	meters, kilogram, seconds
MPP	Massively Parallel Processing
RP #1	Roma Plastilina No. 1 clay
SFA	X-axis scale factor
SFO	Y-axis scale factor

1 (PDF) DEFENSE TECHNICAL INFORMATION CTR DTIC OCA

1 (PDF) DEVCOM ARL FCDD RLD DCI TECH LIB

7 (PDF) DEVCOM SC D COLANTO R DILALLA J FONTECCHIO B FASEL J KIREJCZYK M MAFEO J PARKER

3 (PDF) PROG EXECUTIVE OFC SOLDIER C BAKER J HOPPING J MULLENIX

42 (PDF) DEVCOM ARL FCDD RLC ED S O'BRIEN FCDD RLW S KARNA A RAWLETT S SCHOENFELD J ZABINSKI FCDD RLW B C HOPPEL P GILLICH RC BECKER AL TONGE FCDD RLW MA T BOGETTI S BOYD T PLAISTED J STANISZEWSKI E WETZEL M YEAGER FCDD RLW ME L VARGAS-GONZALEZ FCDD RLW T R FRANCART FCDD RLW TA S BILYK FCDD RLW TB D KRAYTERMAN S ALEXANDER R BANTON T BAUMER B FAGAN A GOERTZ A GUNNARSSON C HAMPTON R KARGUS M KLEINBERGER E MATHEIS J MCDONALD P MCKEE K RAFAELS S SATAPATHY M TEGTMEYER C WEAVER T WEERASOORIYA S WOZNIAK T ZHANG FCDD RLW TD B KRZEWINSKI FCDD RLW TE P SWOBODA FCDD RLW TF J CAZAMIAS FCDD RLW TG N GNIAZDOWSKI